Limnol. Oceanogr., 58(3), 2013, 977–986

doi:10.4319/lo.2013.58.3.0977

Global patterns in oceanic planktonic metabolism

Aurore Regaudie-de-Gioux[a,*] and Carlos M. Duarte[a,b,c]

[a] Department of Global Change Research, Instituto Mediterráneo de Estudios Avanzados (Consejo Superior de Investigaciones Científicas–Universidad de las Islas Baleares), Esporles, Spain

[b] Faculty of Marine Sciences, King Abdulaziz University, Saudi Arabia

[c] The University of Western Australia Oceans Institute and School of Plant Biology, University of Western Australia, Crawley, Western Australia, Australia

Abstract

Rates of gross primary production (GPP) and respiration (CR) of plankton communities in the upper ocean were evaluated on the basis of a data set comprising 3149 paired light and dark bottle measurements of volumetric GPP-CR of euphotic zone plankton communities. The data were from 72 published and unpublished reports of measurements made between 1981 and 2011 from the open ocean and the Mediterranean Sea. The data set is dominated by measurements in chlorophyll *a* (Chl *a*)–rich oceans and North Atlantic waters, with a paucity of measurements in the Indian Ocean and South Pacific Ocean. CR scaled as the 3/4 power of GPP with a power slope of 0.79 ± 0.01, implying that the threshold GPP separating heterotrophic from autotrophic plankton communities is 1.26 mmol O_2 m^{-3} d^{-1}. Plankton communities with Chl $a < 0.35$ mg m^{-3} tend to be heterotrophic. Both GPP and CR declined exponentially with depth, but the GPP declined faster, at 42% ± 7% m^{-1}, than CR (29% ± 8% m^{-1}), so that CR increases relative to GPP with depth.

Marine pelagic ecosystems contribute approximately half of the Earth's photosynthetic production, supported by only 0.2% of the Earth's photosynthetic biomass (Falkowski 1994; Antoine et al. 1996; Behrenfeld and Falkowski 1997; Field et al. 1998). In contrast to the dominance of autotrophic biomass on land, this small photosynthetic biomass supports a comparatively larger biomass of heterotrophs in the ocean (Gasol et al. 1997), which is associated with a high heterotrophic activity in oceanic plankton communities (Duarte and Cebrián 1996; Duarte and Agustí 1998; del Giorgio and Williams 2005; Robinson and Williams 2005). Indeed, planktonic respiration may exceed primary production in individual plankton communities, particularly in the oligotrophic ocean (Duarte and Agustí 1998; Duarte and Prairie 2005; Duarte and Regaudie-de-Gioux 2009). The suggestion that heterotrophic communities (i.e., where the rate of community respiration [CR] is greater than the rate of gross primary production [GPP]) may prevail in oligotrophic ocean ecosystems raised considerable debate (Karl et al. 1993; Williams and Bower 1999; del Giorgio and Duarte 2002; Duarte et al. 2013; Williams et al. 2013). However, this controversy proved positive and stimulated much-needed research to expand the meager empirical basis (del Giorgio and Williams 2005) on which these debates were originally based (Duarte et al. 1999; Williams and Bower 1999; del Giorgio and Duarte 2002).

A first major step in assessing planktonic respiration at the global scale was a review of marine plankton metabolism (Robinson and Williams 2005), which reported 957 paired observations of volumetric plankton metabolism and respiration (cf. fig. 9.10 in Robinson and Williams 2005). These data were dominated by estimates derived from midlatitudes in the Atlantic Ocean, with very few estimates available for the rest of the ocean (cf. figs. 9.2 and 9.12 in Robinson and Williams 2005). The resulting geographically limited data set precluded a robust evaluation of global and regional patterns in planktonic metabolism.

The possible prevalence of heterotrophy in some oceanic communities requires allochthonous inputs of organic carbon (del Giorgio and Duarte 2002; Duarte and Prairie 2005), which may derive from riverine inputs and atmospheric deposition (del Giorgio and Duarte 2002; Duarte et al. 2013). Riverine inputs enter the ocean through the coastal margins and are not evenly distributed in the ocean, with the Arctic Ocean receiving about 3000 km^3 yr^{-1} of freshwater runoff (Carmack and Wassmann 2006), and the equatorial western Atlantic receiving 70,140 km^3 yr^{-1} of freshwater just from the Amazon and Orinoco rivers (Franzinelli and Potter 1983; Lewis et al. 1990). Likewise, atmospheric inputs of organic carbon appear to be highest in the tropical ocean, particular in the eastern Atlantic Ocean (Dachs et al. 2005; Jurado et al. 2008). In addition, respiratory activity is likely to be elevated relative to primary production in warm tropical ocean waters (López-Urrutia et al. 2006; Regaudie-de-Gioux and Duarte 2012). Hence, plankton metabolism is expected to exhibit significant variability across the ocean.

Plankton community metabolism has been addressed using a diversity of techniques, including oxygen evolution in dark–light bottles (Carpenter 1965; Carrit and Carpenter 1966); tracer additions (^{14}C additions, Steeman Nielsen 1952; ^{18}O-labeled H_2O, Bender et al. 1987); incubation-free methods, including analyses of triple oxygen isotopes (Luz and Barkan 2000); O_2 : Ar ratios (Emerson 1987; Spitzer and Jenkins 1989; Emerson et al. 1993); nonintrusive bio-optical methods (Claustre et al. 2008); fast–repetition-rate fluorometry (Kolber and Falkowski 1993); and oxygen sensors mounted on gliders (Tengberg et al. 2006;

* Corresponding author: aurore.regaudie@imedea.uib-csic.es

Nicholson et al. 2008) and buoys (Boutin and Merlivat 2009). The estimates derived from each of these methods are not directly comparable, as they have different assumptions and limitations, and often address different processes (Marra 2002; Robinson and Williams 2005; Robinson et al. 2009; Duarte et al. 2013). A large data set compiling plankton metabolism rates derived from these different methods is available from the digital repository of the Spanish Council for Scientific Research (Regaudie-de-Gioux and Duarte 2013), where the data set will be maintained and expanded in the future. Most estimates of GPP, R, and net community production (NCP) available in this data set were derived using the dark–light method (83%, 100%, and 97%, respectively), with the rest of the techniques providing a limited number of estimates and a limited geographic coverage. Hence, as Robinson and Williams (2005), we focused this review on estimates derived using the dark–light method. Our expanded dark–light data set includes 3854 measurements of light and dark bottle volumetric metabolic rates derived from 1395 stations across the ocean with 3149 paired GPP–CR volumetric data. We examined the distribution of volumetric rates of planktonic GPP, CR, NCP (= GPP − CR), and the ratio of GPP to CR (P : R ratio); the depth distribution and relationships between CR and GPP for the global data set; differences in GPP between autotrophic and heterotrophic planktonic communities; and the thresholds of GPP and chlorophyll *a* (Chl *a*) separating these communities.

Methods

We used here Robinson and Williams's (2005) metabolism data comprising GPP and CR, and we expanded it to include recently published data and our own unpublished data using the dark–light technique from 72 individual reports published between 1981 and 2011 from stations across the open ocean, including the Mediterranean Sea (Table 1). Characteristics of the dark–light method are discussed by Robinson and Williams (2005) and Duarte et al. (2013). The present analysis contains 3854 estimates of volumetric metabolic rates derived from 1395 stations across the ocean with 3149 paired GPP–CR volumetric rate estimates. This restricted data set is available in the Web Appendix (www.aslo.org/lo/toc/vol_58/issue_3/0977a.html).

Depth-integrated rates, calculated using a conventional trapezoid method, were estimated for stations where rates were available for at least three depths within the euphotic layer. However, information in the papers from which data were obtained was not sufficient to integrate to a similar reference depth for all the stations; some integrated across the mixed layer, others over the euphotic layer, and others to standard depths. Because the integration to varying reference depths could introduce biases, we present integrated mean rates (Table 2), with the individual estimates reported in the Web Appendix.

Concurrent measurements of Chl *a* concentration and bacterial abundance were included in the data set where available. Photosynthetically available radiation (PAR) data were not available for most of the database. Where PAR was not reported, we extracted cloud-corrected surface PAR data (Einstein m^{-2} d^{-1}) from the Sea-viewing Wide Field-of-view Sensor (SeaWiFS; McClain et al. 1998) for each station and the corresponding sampling date, which are included in the Web Appendix.

Mean values and parametric statistics were used to report statistics for variables normally distributed in the data set and with equal variance (*f*-test), and nonparametric statistics were used otherwise. The uncertainty of the estimates was reported for only about two-thirds of the estimates, so the precision of some of the estimates could not be assessed. Future reports of plankton metabolic rates should provide error estimates for rates so that new global analyses can fully account for the precision of the estimates. The central tendency of the P : R ratio was represented by the median value, because the mean value is biased towards values > 1 (e.g., the mean P : R of two communities, one where GPP = 2 CR, and another one where GPP = 1/2 CR is 1.25). Model II regression was used to represent the relationship between variables, which were log transformed when necessary to comply with the requirements of the analysis.

The robustness of the relationship between CR and GPP derived from the 3149 volumetric GPP–CR paired estimates across the ocean was tested using bootstrap. Specifically, we randomly selected 10% paired observations of CR and GPP from the dark–light data set, then fitted a linear regression Type II model to the log-transformed rates, calculated the threshold of GPP for GPP = CR using a logistic regression to the log-transformed rates, and used the fitted Type II model regression equation to predict the CR values for the observations not used to fit the regression from the corresponding GPP to test the predictive power of the regression equation. We repeated this procedure 10 times to examine the variability of the parameters and their possible dependence on specific subsets of data.

Results

The dark–light database provides an improved global coverage of planktonic metabolism in the ocean (Table 1; Figs. 1, 2). Most of the observations derive from the Atlantic Ocean (Figs. 1, 2), with a relatively high density of data also available for the Antarctic Peninsula in the Southern Ocean, eastern Arctic Ocean, and Mediterranean Sea (Table 1; Figs. 1, 2). In contrast, there is still a remarkable paucity of data in the Pacific Ocean and the Indian Ocean (Figs. 1, 2). Dark–light method planktonic metabolism measurements began increasing in the early 1990s, to 545 observations between 2007 and 2010 (Fig. 3).

The highest Chl *a* concentrations (> 1.5 mg Chl *a* m^{-3}; Table 3) in the dark–light data set were observed for stations sampled in the Arctic and Southern Ocean (*t*-test, $t = 2.32$, df = 1455, $p < 0.05$ and $t = 8.02$, df = 1485, $p < 0.05$, respectively) and the lowest were for stations in the Mediterranean Sea and Pacific and Indian Oceans ($<$ 0.7 mg m^{-3}; Table 3). Bacterial abundances in the dark–light data set for stations sampled in the Mediterranean Sea were significantly lower than in the Arctic and Atlantic Ocean (*t*-test, $t = -2.44$, df = 530, $p < 0.05$ and $t = -2.84$,

Table 1. Sources of data for the dark–light database on plankton metabolism in the upper ocean, including the number of observations (*n* data) (references available in the Web Appendix).

Ocean	Reference	*n*
Atlantic	Aranguren-Gassis et al. 2011*	31
	Aranguren-Gassis et al. 2012*	56
	Arístegui and Harrison 2002	40
	Arístegui et al. 2004	22
	Arístegui unpubl. (1991; 2000)*	13
	Aristegui et al. 2009	96
	Gist et al. 2009	161
	González et al. 2001	64
	González et al. 2002	117
	González et al. 2003	12
	Lowry 2004†	151
	Maixandeau et al. 2005	242
	Morán et al. 2004	36
	Mouriño-Carballido and McGillicuddy 2006	31
	Mouriño-Carballido and Anderson 2009	10
	Navarro et al. unpubl. data 2003	79
	Regaudie-de-Gioux and Duarte 2010*b*	71
	Robinson unpubl. 2004‡	13
	Robinson unpubl.*	4
	Robinson et al. 2009	29
	Serret et al. 1999	45
	Serret et al. 2001*b*	19
	Serret et al. 2001*b*; Robinson et al. 2002‡	118
	Serret et al. 2006	95
	Teira et al. 2001	31
	Williams 1998; Williams 2000‡	143
Pacific	Godoy et al. 2012	18
	Hashimoto et al. 2006	21
	Karl and Church§	18
	MacAndrew et al. 2007	9
	Sarma et al. 2005	6
	Sarma et al. 2008	18
	Viviani et al. 2011	13
	Williams and Purdie 1991	15
	Williams et al. 2004	178
Mediterranean Sea	Bonilla-Findji et al. 2010	49
	Duarte et al. 2000	3
	Duarte et al. 2004	334
	González et al. 2008	32
	Lefèvre unpubl. 2004*	65
	Lefèvre et al. 1997	83
	Lucea et al. 2005	24
	Navarro et al. 2004	15
	Regaudie-de-Gioux et al. 2009	69
	Robinson 2000	17
	Satta et al. 1996	25
Antarctic	Agustí et al. 2004	22
	Agustí and Duarte 2005	4
	Arístegui et al. 1996	22
	Bender et al. 2000; Marra 2002	61
	Bender 2003†	144
	Blight 1996*	17
	Bouquegneau et al. 1992	14
	Boyd et al. 1995‡	16
	Dickson and Orchado 2001; Marra 2002	125
	Lefèvre et al. 2008	42
	Navarro et al. unpubl. data 2005	33
	Odate et al. 2002	12
	Regaudie-de-Gioux unpubl. data 2009	77
	Robinson unpubl. 1997*	11
	Robinson and Williams 1993	11
	Serret et al. 2001*a*†	20
Indian	Lowry 2004†	27
	Robinson 2003†	40
	Robinson and Williams 1999‡	40
Arctic	Cottrell et al. 2006	112
	Holligan et al. 1984	22
	Regaudie-de-Gioux and Duarte 2010*a*	66
	Robinson et al. 2002‡	35
	Vaquer-Sunyer et al. 2013	140
Total		3854

* Data from Robinson and Williams (2005).
† Data held at Data Published for Earth and Environmental Science PANGAEA data collection.
‡ Data also held at the British Oceanographic Data Centre (www.bodc.ac.uk).
§ CMORE data online at http://cmore.soest.hawaii.edu/.

df = 530, $p < 0.05$, respectively) (Table 3). The majority of the Chl *a* values (48%) were within the range 0.25 to 1.6 mg Chl *a* m^{-3} and 25% of the values were in the range 0.40 to 1 mg Chl *a* m^{-3}, suggesting that high–Chl *a* communities are overrepresented in the database available on plankton community metabolism rate, because most of the Chl *a* values in ocean surface waters are between 0.08 and 0.6 mg Chl *a* m^{-3} (Morel and Maritorena 2001). Indeed, the median Chl *a* concentration was 0.49 mg Chl *a* m^{-3} and 45% of the Chl *a* values in our dark–light data set were above 0.6 mg Chl *a* m^{-3}. Examination of the geographic spread of stations supports this suggestion, as the oligotrophic gyres of the subtropical ocean, which comprise 70% of the ocean surface, are underrepresented, particularly in the Indian and Pacific Oceans (Fig. 1).

The geographical coverage of dark–light method data is improved relative to previous compilations, but the distribution across the ocean remains sparse and imbalanced (Fig. 1). Whereas coverage is relatively high for the Atlantic Ocean (Table 3; Fig. 1), all other oceans remain grossly undersampled. Hence, mean metabolic rates, whether global or basin specific, are likely biased estimates of the true global and regional mean values. For the dark–light method data set, the mean volumetric GPP rates (3.8 $\pm$ 0.5 mmol O_2 m^{-3} d^{-1}) were significantly higher (*t*-test, $t = 11.09$, df = 3183, $p < 0.05$) than the mean volumetric CR rates (2.2 $\pm$ 1.0 mmol O_2 m^{-3} d^{-1}; Table 2). Accordingly, the mean volumetric NCP rate (1.2 $\pm$ 0.8 mmol O_2 m^{-3} d^{-1}) was significantly higher than 0 (*t*-test, $t = 11.26$, df = 3521, $p < 0.05$; Table 2) and the median volumetric P : R ratios was 1.1 $\pm$ 2.3 (Table 2), indicative of a balance between autotrophic and heterotrophic metabolism.

The highest metabolic rates, averaging 6.6 $\pm$ 0.6 and 2.6 $\pm$ 0.8 mmol O_2 m^{-3} d^{-1}, respectively, were in the top 10 m. Indeed, metabolic rates declined exponentially with depth (Fig. 4), with GPP declining faster (42% $\pm$ 7% m^{-1}) than CR (29% $\pm$ 8% m^{-1}) with depth. This confirms that the ratio P : R tends to decline with depth, i.e., communities become more heterotrophic as depth increases (Duarte et al. 2013).

Table 2. Volumetric (mmol O_2 m^{-3} d^{-1}) and integrated (mmol O_2 m^{-2} d^{-1}) mean (± SE), range (minimum–maximum), and number of observations of GPP, CR, and NCP, and the median (± SE), range (minimum–maximum), and number of observations of P : R ratio for stations where the planktonic metabolism rates were evaluated by the dark–light method. The error propagation was calculated and is signalized by an asterisk.

	GPP	CR	NCP	P : R	% heterotrophic rates
Integrated (±SE)	114.1±5.0	96.9±4.3	17.5±5.0	1.1±0.1	45%
Range	0–972.3	0–1122.8	−1056.6–1118.1	0–33.1	
n	647	690	697	578	
Volumetric (±SE)	3.8±0.5*	2.2±1.0*	1.2±0.8*	1.1±2.3*	47%
Range	0–399	0–44.6	−38.7–81.6	0–543	
n	3335	3437	3520	3174	
Volumetric surface water (<10 m) (±SE)	6.6±0.6*	2.6±0.8*	2.9±0.6*	1.5±1.9*	32%
Range	0–399	0–40.9	−18.5–69.7	0–344	
n	893	873	965	740	

The minimum value of surface irradiance was observed for stations sampled in the Arctic Ocean (1.4 Einstein m^{-2} d^{-1}) and the maximum value for stations sampled in the Atlantic Ocean (62.6 Einstein m^{-2} d^{-1}) (data available in the Web Appendix). The integrated GPP and CR rates showed a weak but significant tendency to increase with the surface irradiance (PAR) (Fig. 5), with this relationship being, unexpectedly, stronger for CR than for GPP (for integrated GPP, $R^2 = 0.06$, $p < 0.05$; for integrated CR, $R^2 = 0.17$, $p < 0.05$). No significant relationship ($p > 0.05$) between the depth-integrated NCP and incident PAR was observed.

Volumetric GPP was significantly higher for autotrophic communities (5.42 ± 0.20 mmol O_2 m^{-3} d^{-1}) compared to heterotrophic ones (1.22 ± 0.05 mmol O_2 m^{-3} d^{-1}, *t*-test, $t = -20.96$, df = 1927, $p < 0.001$) and volumetric CR was significantly lower for autotrophic communities (1.95 ± 0.05 mmol O_2 m^{-3} d^{-1}) than for heterotrophic ones (2.58 ± 0.09 mmol O_2 m^{-3} d^{-1}, *t*-test, $t = 6.13$, df = 2643, $p < 0.001$).

Logistic regression was used to derive the threshold GPP separating autotrophic from heterotrophic communities, which was estimated at 1.26 mmol O_2 m^{-3} d^{-1} (χ^2 test, $p < 0.0001$).

Autotrophic communities had higher Chl *a* concentration (1.61 ± 0.10 mg Chl *a* m^{-3} vs. 0.71 ± 0.06 mg Chl *a* m^{-3}, *t*-test, $t = -8.04$, df = 1126, $p < 0.001$) and bacterial abundance (0.89 ± 0.05 × 10^6 cell mL^{-1} vs. 0.68 ± 0.03 × 10^6 cell mL^{-1}, *t*-test, $t = -3.51$, df = 382, $p < 0.001$) than

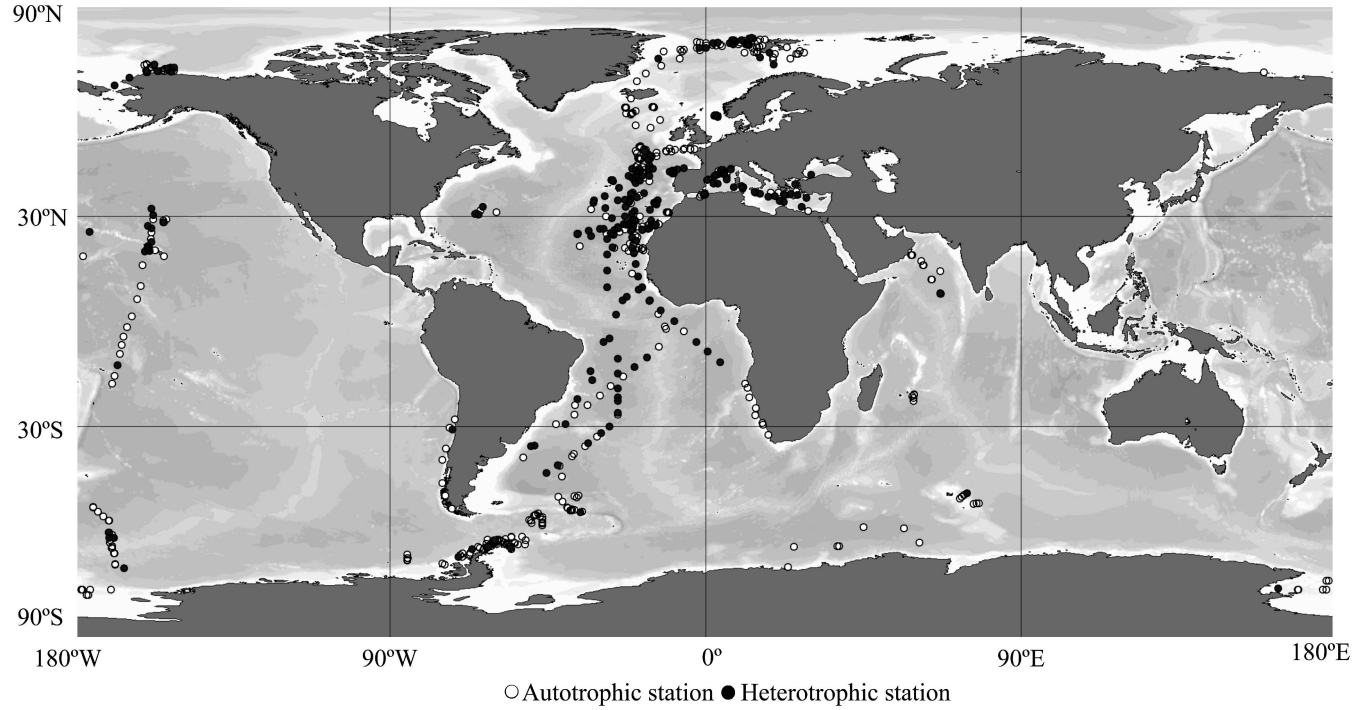

Fig. 1. Geographical distribution of the different stations where the planktonic metabolism has been measured by the dark–light method. White and black circles represent autotrophic and heterotrophic stations, respectively.

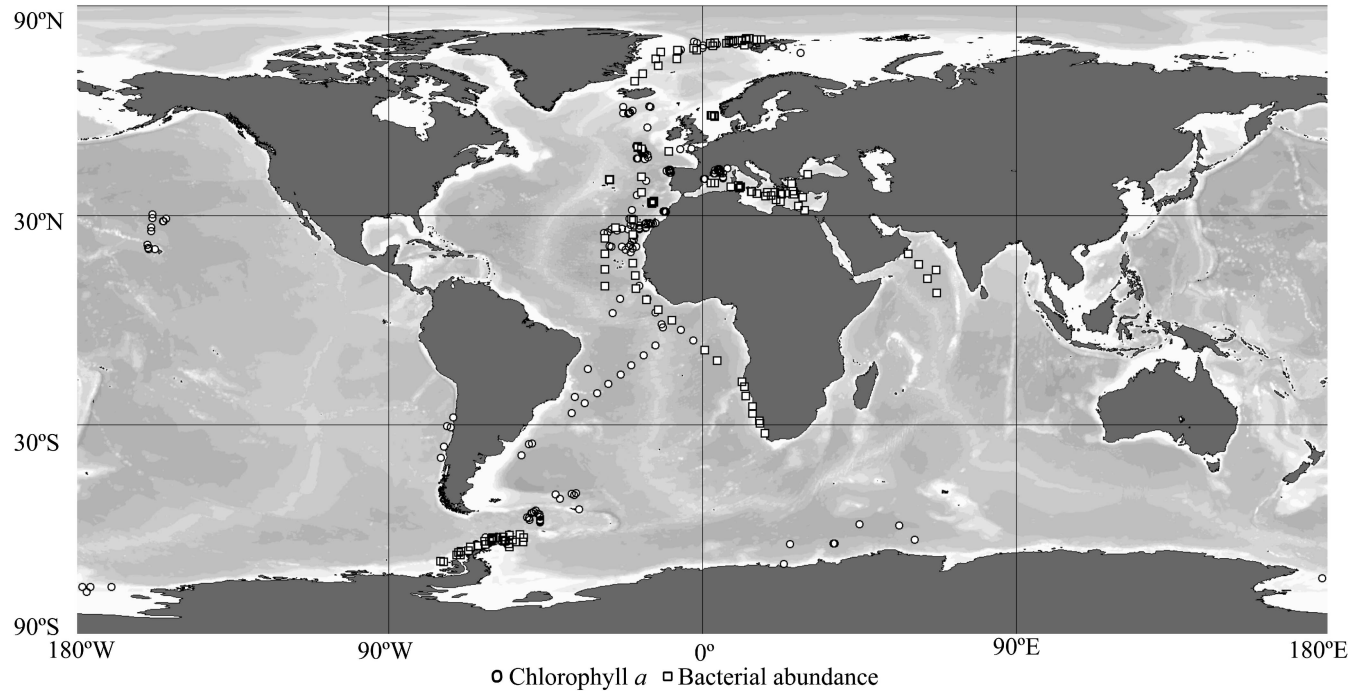

Fig. 2. Geographical distribution of the different metabolism stations measured by the dark–light method where the Chl *a* (circles) and the bacterial abundance (squares) data were available.

heterotrophic ones. Fitted logistic regression was used to derive the threshold Chl *a* separating autotrophic from heterotrophic communities, which was found to be 0.35 mg Chl *a* m^{-3} (χ^2 test, $p < 0.0001$). GPP rates increased significantly with increasing Chl *a*, although the relationship was relatively weak (Fig. 6), as described by the fitted model II regression equation:

$$\text{Log GPP(mmol O}_2\ \text{m}^{-3}\ \text{d}^{-1}) = 0.53(\pm 0.02) + 1.02(\pm 0.03)\log \text{Chl } a(\text{mg m}^{-3}) \quad (1)$$
$$(R^2 = 0.29,\ p < 0.05,\ n = 1111)$$

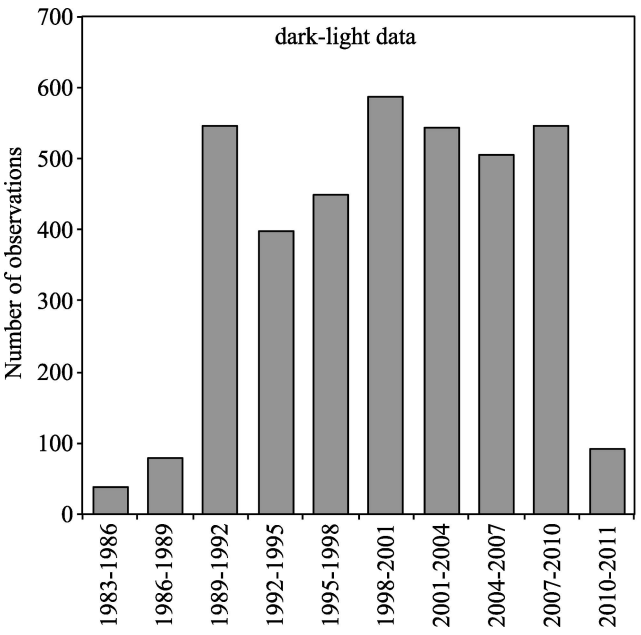

Fig. 3. Yearly distribution of the number of observations of planktonic metabolism measured by the dark–light method in the open ocean.

The slope being close to 1.0 shows that GPP increases proportionally to Chl *a*. Similarly, NCP and CR rates increased significantly with increasing Chl *a* ($R^2 = 0.23$ and 0.09, respectively, $p < 0.05$), but these relationships were even weaker than that for GPP (data not shown here). Volumetric CR rates tended to increase with increasing bacterial abundance (Fig. 6), but the relationship was very weak ($R^2 = 0.05$, $p < 0.05$). Volumetric GPP tended to weakly increase with increasing bacterial abundance ($R^2 = 0.09$, $p < 0.05$) whereas no significant relationship between NCP rates and bacterial abundance was observed ($R^2 = 0.02$, $p > 0.05$) (data not shown here).

CR rates increased with increasing GPP (Fig. 6) as described by the fitted model II regression equation:

$$\text{Log CR(mmol O}_2\ \text{m}^{-3}\ \text{d}^{-1}) = 0.01(\pm 0.01) + 0.79(\pm 0.01)\log \text{GPP(mmol O}_2\ \text{m}^{-3}\ \text{d}^{-1}) \quad (2)$$
$$(R^2 = 0.30,\ p < 0.05,\ n = 3149)$$

The slope being significantly < 1 (*F*-test, $t = 1$, df = 3182, $p < 0.05$) indicates that CR increases as the 3/4 power of GPP and is, therefore, highest relative to GPP in communities with low GPP. Some GPP and CR data (5% and 3% of the estimates in the dark–light database, respectively) were reported to be below 0.1 mmol O_2

Table 3. Mean (± SE) of Chl *a* concentration, bacterial abundance, and PAR from SeaWiFS (number of observations) for stations at five different oceans and the Mediterranean Sea where the planktonic metabolism rates were evaluated by the dark–light method. nd, not determined.

	Global ocean	Atlantic Ocean	Pacific Ocean	Indian Ocean	Arctic Ocean	Southern Ocean	Mediterranean Sea
Chl *a* (mg m^{-3})	1.2±0.1(1300)	0.8±0.0(625)	0.5±0.1(43)	0.5±0.0(38)	1.7±0.2(155)	2.8±0.3(243)	0.5±0.1(196)
Bacterial abundance (10^6 cell mL^{-1})	0.8±0.0(535)	0.8±0.0(225)	nd	0.9±0.0(29)	0.8±0.1(110)	0.7±0.1(94)	0.6±0.0(77)
PAR (Einstein m^{-2} d^{-1})	37.7±0.4(1389)	40.8±0.5(705)	46.4±1.1(173)	nd	34.1±1.7(118)	24.0±0.8(268)	40.9±1.9(125)

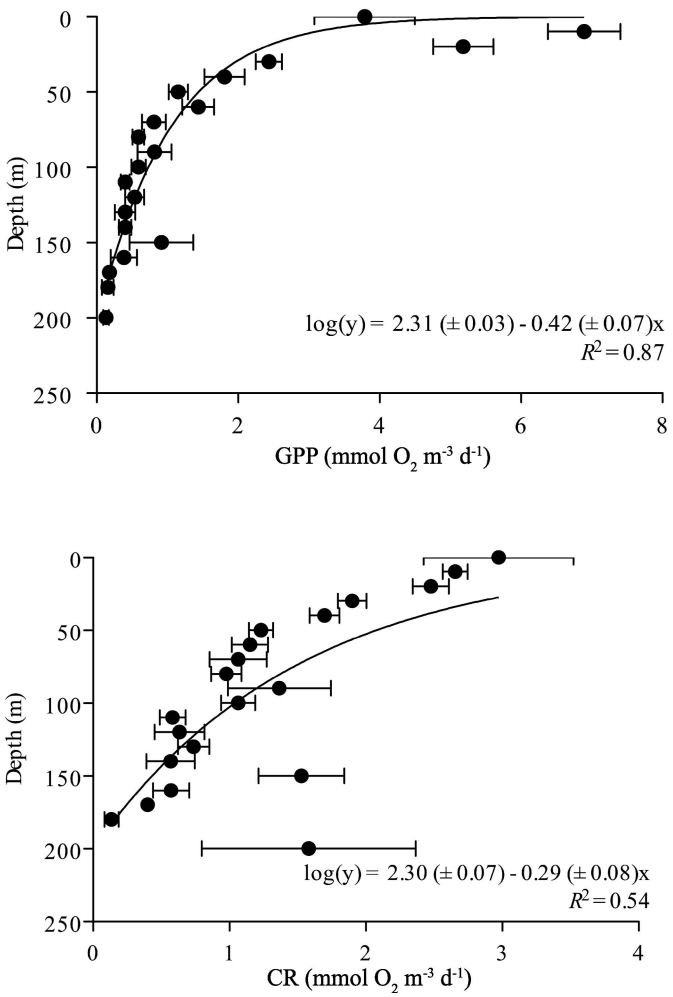

Fig. 4. Relationship between the average ± SE volumetric GPP and CR (mmol O_2 m^{-3} d^{-1}) both measured by the dark–light method within 10 m depth bins and the depth (m). The solid lines represent the fitted semilog-line regression with equations reported in the figure.

m^{-3} d^{-1}, which is close to the detection limit, possibly affecting the regression between CR and GPP. However, the slope of the log CR vs. log GPP regression had a slope of 0.79 ± 0.01, an intercept of −0.002 ± 0.01, and a threshold of GPP of 1.33 when these data were excluded. These regression parameters and threshold of GPP were not significantly different (*t*-test, $t = 0.43$, df = 10, $p > 0.05$) from those derived for the entire dark–light data, showing that GPP and CR rates < 0.1 mmol O_2 m^{-3} d^{-1} did not significantly influence the regression analysis.

We used bootstrap to examine the variability of the estimates and the robustness of the representation derived from the dark–light data set assembled. The bootstrap estimates of slope, intercept, and threshold of GPP showed little variability and were not significantly different (*t*-test, $t = 0.43$, df = 10, $p > 0.05$) from the regression parameters derived using the entire dark–light data (Table 4). The bootstrap results demonstrated the robustness of the relationship and showed that this relationship provides an adequate representation of the functional regression

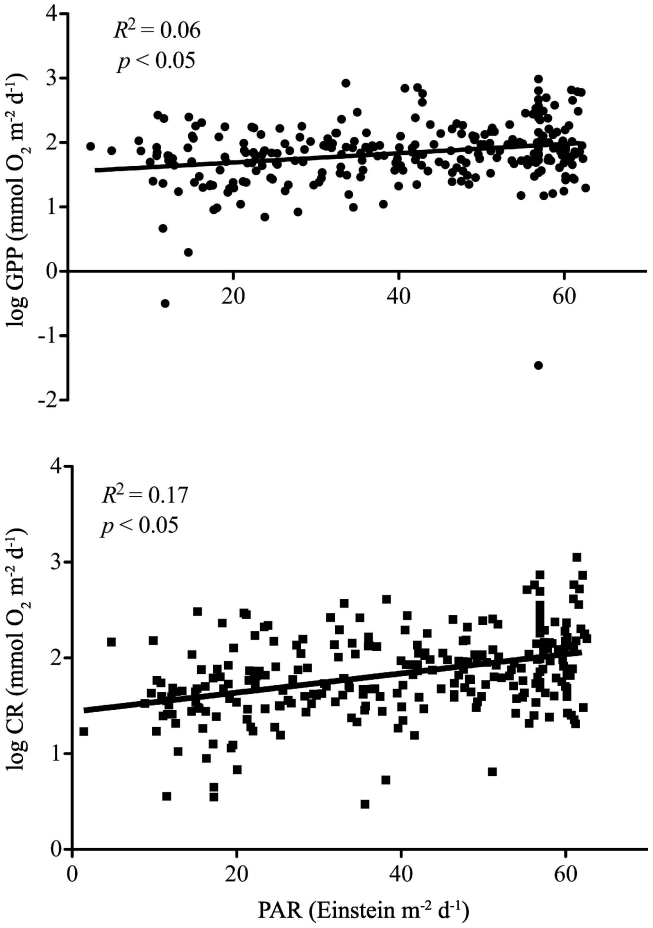

Fig. 5. Log–log plot of integrated GPP (mmol O_2 m^{-2} d^{-1}) and integrated CR (mmol O_2 m^{-2} d^{-1}) both measured by the dark–light method with surface irradiance (PAR, Einstein m^{-2} d^{-1}). The fit model I regressions have the following equation: log GPP = 1.55 (± 0.07) + 0.007 (± 0.002) PAR, $R^2 = 0.06$, $p < 0.05$, $n = 268$; log CR = 1.44 (± 0.06) + 0.01 (± 0.001) PAR, $R^2 = 0.17$, $p < 0.05$, $n = 274$.

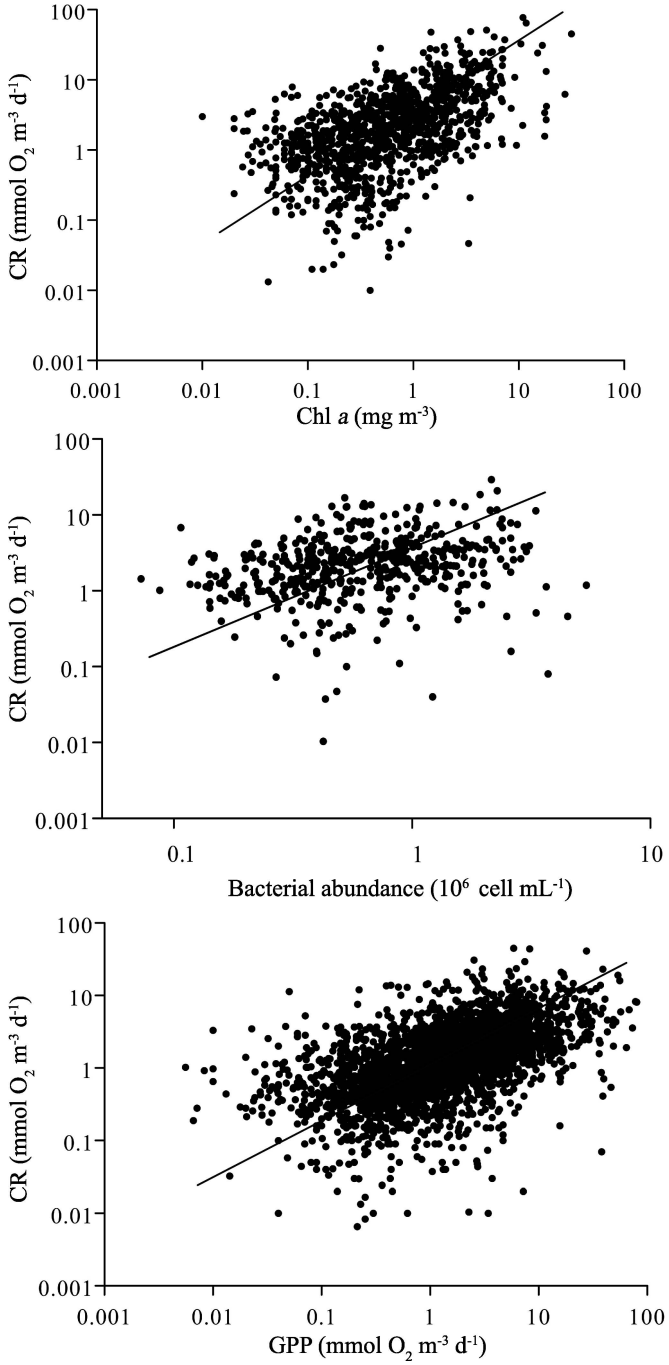

Fig. 6. Log–log plot of GPP (mmol O_2 m^{-3} d^{-1}) and Chl *a* (mg m^{-3}), CR (mmol O_2 m^{-3} d^{-1}) and bacterial abundance (BA, cell mL^{-1}), and GPP (mmol O_2 m^{-3} d^{-1}) and CR (mmol O_2 m^{-3} d^{-1}) from the dark–light method data set. The fitted model II regressions have the following equations: log GPP = 0.53 (± 0.02) + 1.02 (± 0.03) log Chl *a*, $R^2 = 0.29$, $p < 0.05$, $n = 1111$; log CR = −7.20 (± 0.33) + 1.30 (± 0.06) log BA, $R^2 = 0.05$, $p < 0.05$, $n = 493$; log CR = 0.79 (± 0.01) log GPP + 0.01 (± 0.01), $R^2 = 0.30$, $p < 0.05$, $n = 3149$.

between CR and GPP across the ocean, not contingent on the specific data used. Bootstrap also showed the GPP threshold for GPP = CR to be robust (Table 4), and to correctly classify as heterotrophic or autotrophic on average 63.2% ± 0.3% of independent communities.

Discussion

The results presented are based on a much-expanded data set (3854 community rates, 3149 volumetric GPP–CR paired estimates, and 1395 individual stations) of metabolic rates by plankton communities measured by the dark–light method in the photic zone of the ocean compared to previous efforts (Robinson and Williams 2005). In addition to the increased sample size, the present dark–light database encompasses communities sampled in the five different oceans and the Mediterranean Sea, for different periods of the year. This represents an improvement relative to previous assessments, such as that of Robinson and Williams (2005) dominated by estimates derived from midlatitudes in the Atlantic Ocean, with very few estimates available for the rest of the ocean (cf. figs. 9.2 and 9.12 in Robinson and Williams 2005). Despite these improvements, the dark–light data set on plankton metabolic rates

Table 4. Mean (± SE) of the log CR vs. log GPP regression analysis deviation (slope, intercept, R^2, and threshold) using all the data of the dark–light data set and derived using bootstrap estimates. The mean (± SE) of the bootstrap estimates represents that of 10 bootstrapping iterations.

	All data (mean±SE)	Bootstrapping estimates (mean±SE)
Slope	0.79±0.01	0.76±0.10
Intercept	0.01±0.01	0.02±0.01
R^2	0.30	0.30±0.06
Threshold	1.26	1.29±0.10

analyzed is still highly imbalanced, with a dominance of stations sampled in coastal and North Atlantic waters (45% of all measurements), and particularly poor representation of the South Pacific and South Indian Oceans. Because the distribution of communities in the data set is biased towards productive ones, the average values cannot be directly extrapolated to derive global estimates of GPP and respiration of planktonic communities nor the metabolic balance of the ocean.

We are, thus, still far from achieving a globally balanced representation of metabolic rates in the global ocean despite a major increase in rates available. However, this analysis can directly help the research community contributing to this topic into targeting the underrepresented regions, thereby helping build a database eventually allowing scaling of a true global picture of ocean metabolism. Efforts should concentrate in the southern hemisphere, as the ocean surface : land surface ratio there (1 : 4) is much greater than that in the northern hemisphere, which has a ratio of about 1 : 1.5.

The relationship between GPP and Chl *a* concentration reported here could possibly provide an avenue to scale up GPP at the global scale from Chl *a* concentration. However, this relationship accounts for only 30% of the variance in GPP, indicating that predicting GPP from Chl *a* concentration involves considerable uncertainty, and that factors other than Chl *a* concentration, including irradiance (Copeland 1965; Goldsborough and Kemp 1988), temperature (Brown et al. 2004; López-Urrutia et al. 2006; Regaudie-de-Gioux and Duarte 2012), and nutrient concentration (Oviatt et al. 1993; Taylor et al. 1995), among others, must play an important role in regulating planktonic GPP. Whereas we observed that the integrated GPP was only weakly correlated with the incident surface irradiance (Fig. 5), temperature has been reported to exert a strong effect on Chl *a*–specific metabolic rates, with specific respiration rates increasing steeply with increasing temperature (Regaudie-de-Gioux and Duarte 2012). Indeed, evaluation of the temperature dependence of plankton community metabolism has shown that, as predicted from metabolic theory (Harris et al. 2006), CR increases faster than GPP, with the activation energy in the Arrhenius equation describing the temperature dependence of CR, 0.66 ± 0.05 eV, being twice as high as that for GPP, 0.32 ± 0.04 eV (Regaudie-de-Gioux and Duarte 2012). Accordingly, the P : R ratio increases with increasing temperature, and communities in waters warmer than 21°C tend to have P : R ratios < 1 (Regaudie-de-Gioux and Duarte 2012). Moreover, the global inventory of Chl *a* concentration is available only for surface waters, which are accessible to satellite-based instruments, and thus does not allow integration of GPP across the entire photic layer.

Our results confirm that the respiration of planktonic communities of our dark–light data set increases with increasing GPP (Fig. 6). However, CR scaled as the 0.79 ± 0.01 power of GPP for our dark–light data set, compared to the 0.5 ± 0.03 power reported by Duarte and Agustí (1998) and the 0.62 power reported by Robinson and Williams (2005). Bootstrap analyses showed that the slope of 0.79 ± 0.01 reported here is robust, so that the doubling of metabolic rates included in our analysis relative to earlier effort now provides a robust representation of the functional scaling between CR and GPP. CR increasing as the 3/4 power of GPP indicates that, as observed in the past, CR increases more slowly with increasing GPP than GPP does, i.e., unproductive communities tend to have low P : R ratios (Duarte and Agustí 1998). Differences in the scaling of GPP to CR may occur, depending on the allochthonous inputs of organic carbon to the communities, which may elevate CR relative to GPP (i.e., higher intercept), particularly at low GPP (i.e., shallow slopes), as well as water temperature, which results in elevated CR for a given GPP in warm surface waters (Regaudie-de-Gioux and Duarte 2012).

Our results also confirm earlier indications that communities with low GPP and low Chl *a* concentrations tend to be heterotrophic (Duarte and Agustí 1998). The threshold GPP of 1.26 mmol O_2 m^{-3} d^{-1} reported here is within the range of previous estimates (Duarte and Regaudie-de-Gioux 2009), but somewhat higher than those derived from previous global analyses (1.06 mmol O_2 m^{-3} d^{-1}, Duarte and Agustí 1998; 1.09 mmol O_2 m^{-3} d^{-1}, Robinson and Williams 2005).

Half of the sampled dark–light communities were heterotrophic (Table 2). However, the fraction of heterotrophic communities in our analysis is likely underestimated because the least productive regions of the ocean, the southern subtropical gyres, are grossly underrepresented in the data set. Indeed, the threshold Chl *a* concentration of 0.35 mg Chl *a* m^{-3} separating heterotrophic from autotrophic communities is higher than the median Chl *a* concentration in open ocean waters (Morel and Maritorena 2001), suggesting that heterotrophic communities may prevail in the open ocean. Furthermore, 78% of the annual surface satellite Chl data (SeaWiFS data) in 1998 and 76% in 2008 were below the threshold Chl *a* concentration, suggesting that heterotrophic communities should prevail in the surface of the open ocean. Resolving the metabolic balance of the ocean remains an elusive goal that awaits an effort to improve the distribution of data on metabolic rates in the ocean, particularly for oligotrophic gyres in the southern hemisphere. Likewise, understanding the prevalence of heterotrophic communities in the less productive regions of the ocean requires that allochthonous organic inputs be quantified as a necessary step to reconcile the carbon budget of these important regions of the ocean. In general, although CR is closely coupled to GPP, systems become increasingly autotrophic with increasing GPP.

Our analysis indicates that CR is scaled as the 3/4 power of GPP, with a power slope significantly higher than previous assessments (Duarte and Agustí 1998; Robinson and Williams 2005). This inconsistency is most likely due to biases in the data coverage of the oceans even in the present expanded database. To obtain definitive global values for community metabolism will require a targeted approach using similar techniques focused on the oligotrophic gyres of the South Pacific and the Indian Ocean. A combination of techniques, including in vitro and in situ methods, used concurrently and the use of scaling strategies based on relationships between metabolic rates and temperature, Chl *a,* and irradiance have been proposed to help resolve the metabolic budget of the ocean (Duarte et al. 2013).

Acknowledgments

This is a contribution to the "Malaspina 2010" Consolider project funded by the Spanish Ministry of Science and Innovation (CSD2008-00077) and the Metaoceans Marie Curie Early Stage Research Network (019678-2), funded by the Framework Program 6 of the EU. We thank M. Cottrell, D. Kirchman, V. Sarma, P. Williams, P. Serret, E. Fernandez, B. Mouriño, N. Navarro, C. Robinson, R. Vaquer-Sunyer, and S. Agustí for providing data. A. Regaudie-de-Gioux was supported by the Metaoceans project. We thank the Reviews Editor and the reviewers for the constructive assessment of the manuscript.

References

Antoine, D., J. M. André, and A. Morel. 1996. Oceanic primary production: 2. Estimation at global scale from satellite (Coastal Zone Color Scanner) chlorophyll. Global Biogeochem. Cycles **10:** 57–69, doi:10.1029/95GB02832

Behrenfeld, M. J., and P. G. Falkwoski. 1997. Photosynthetic rates derived from satellite-based chlorophyll concentration. Limnol. Oceanogr. **42:** 1–20, doi:10.4319/lo.1997.42.1.0001

Bender, M. L., and others. 1987. A comparison of four methods for determining planktonic community production. Limnol. Oceanogr. **32:** 1085–1098, doi:10.4319/lo.1987.32.5.1085

Boutin, J., and L. Merlivat. 2009. New in situ estimates of carbon biological production rates in the Southern Ocean from CARIOCA drifter measurements. Geophys. Res. Lett. **36:** L13608, doi:10.1029/2009GL038307

Brown, J. H., J. F. Gillooly, A. P. Allen, V. M. Savage, and G. B. West. 2004. Toward a metabolic theory of ecology. Ecology **85:** 1771–1789, doi:10.1890/03-9000

Carmack, E., and P. Wassmann. 2006. Food webs and physical-biological coupling on pan-Arctic shelves: Unifying concepts and comprehensive perspectives. Prog. Oceanogr. **71:** 446–477, doi:10.1016/j.pocean.2006.10.004

Carpenter, J. H. 1965. The accuracy of the Winkler method for dissolved oxygen analysis. Limnol. Oceanogr. **10:** 135–140, doi:10.4319/lo.1965.10.1.0135

Carrit, D. E., and J. H. Carpenter. 1966. Comparison and evaluation of currently employed modifications of the Winkler method for determining dissolved oxygen in seawater. J. Mar. Res. **24:** 286–318.

Claustre, H., Y. Huot, I. Obernosterer, B. Gentili, D. Tailliez, and M. Lewis. 2008. Gross community production and metabolic balance in the South Pacific Gyre, using a non intrusive bio-optical method. Biogeosciences **4:** 463–474, doi:10.5194/bg-5-463-2008

Copeland, B. J. 1965. Evidence for regulation of community metabolism in a marine ecosystem. Ecology **46:** 563–564, doi:10.2307/1934899

Dachs, J., and others. 2005. High atmosphere-ocean exchange of organic carbon in the NE subtropical Atlantic. Geophys. Res. Lett. **32:** L21807, doi:10.1029/2005GL023799

del Giorgio, P. A., and C. M. Duarte. 2002. Respiration in the open ocean. Nature **420:** 379–384, doi:10.1038/nature01165

———, and P. J. le B. Williams. 2005. Respiration in aquatic ecosystems. Oxford Univ. Press.

Duarte, C. M., and S. Agustí. 1998. The CO_2 balance of unproductive aquatic ecosystems. Science **281:** 234–236, doi:10.1126/science.281.5374.234

———, ———, H. Kennedy, and D. Vaqué. 1999. The Mediterranean climate as a template for Mediterranean marine ecosystems: The example of the northeast Spanish littoral. Prog. Oceanogr. **44:** 245–270, doi:10.1016/S0079-6611(99)00028-2

———, and J. Cebrián. 1996. The fate of marine autotrophic production. Limnol. Oceanogr. **41:** 1758–1766, doi:10.4319/lo.1996.41.8.1758

———, and Y. M. Prairie. 2005. Prevalence of heterotrophy and atmospheric CO_2 emissions from aquatic ecosystems. Ecosystems **8:** 862–870, doi:10.1007/s10021-005-0177-4

———, and A. Regaudie-de-Gioux. 2009. Thresholds of gross primary production for the metabolic balance of marine planktonic communities. Limnol. Oceanogr. **54:** 1015–1022, doi:10.4319/lo.2009.54.3.1015

———, ———, J. M. Arrieta, A. Delgado-Huertas, and S. Agustí. 2013. The oligotrophic ocean is heterotrophic. Ann. Rev. Mar. Sci. **5:** 551–569, doi:10.1146/annurev-marine-121211-172337

Emerson, S. 1987. Seasonal oxygen cycles and biological new production in surface waters of the sub-Arctic Pacific Ocean. J. Geophys. Res.: Oceans **92:** 6535–6544, doi:10.1029/JC092iC06p06535

———, P. Quay, and P. A. Wheeler. 1993. Biological productivity determined from oxygen mass-balance and incubation experiments. Deep-Sea Res. I **40:** 2351–2358, doi:10.1016/0967-0637(93)90109-G

Falkowski, P. G. 1994. The role of phytoplankton photosynthesis in global biogeochemical cycles. Photosynth. Res. **39:** 235–258, doi:10.1007/BF00014586

Field, C. B., M. J. Behrenfeld, J. T. Randerson, and P. Falkowski. 1998. Primary production of the biosphere: Interacting terrestrial and oceanic components. Science **281:** 237–240, doi:10.1126/science.281.5374.237

Franzinelli, E., and P. Potter. 1983. Petrology, chemistry and texture of modern river sands. Amazon River system. J. Geol. **78:** 1203–1232.

Gasol, J. M., P. D. del Giorgio, and C. M. Duarte. 1997. Biomass distribution in marine planktonic communities. Limnol. Oceanogr. **42:** 1353–1363, doi:10.4319/lo.1997.42.6.1353

Goldsborough, W. J., and W. M. Kemp. 1988. Light responses of a submersed macrophyte: Implications for survival in turbid tidal waters. Ecology **69:** 1775–1786, doi:10.2307/1941156

Harris, L. A., C. M. Duarte, and S. W. Nixon. 2006. Allometric laws and prediction in estuarine and coastal ecology, Estuar. Coasts **29:** 340–344, doi:10.1007/BF02782002

Jurado, E., J. Dachs, C. M. Duarte, and R. Simó. 2008. Atmospheric deposition of organic and black carbon to the global ocean. Atmos. Environ. **42:** 7931–7939, doi:10.1016/j.atmosenv.2008.07.029

Karl, D. M., G. Tien, J. Dore, and C. D. Winn. 1993. Total dissolved nitrogen and phosphorous concentrations at U.S.-JGOFS Station ALOHA: Redfield reconciliation. Mar. Chem. **41:** 203–208, doi:10.1016/0304-4203(93)90120-D

Kolber, Z., and P. G. Falkowski. 1993. Use of active fluorescence to estimate phytoplankton photosynthesis in situ. Limnol. Oceanogr. **38:** 1646–1665, doi:10.4319/lo.1993.38.8.1646

Lewis, W. M., F. H. Weibezahn, J. F. Saunders, III, and S. K. Hamilton. 1990. The Orinoco River as an ecological system. Interciencia **15:** 346–357.

López-Urrutia, A., E. San Martin, R. P. Harris, and X. Irigoyen. 2006. Scaling the metabolic balance of the oceans. Proc. Natl. Acad. Sci. USA **103:** 8739–8744, doi:10.1073/pnas.0601137103

Luz, B., and E. Barkan. 2000. Assessment of oceanic productivity with the triple-isotope composition of dissolved oxygen. Science **288:** 2028–2031, doi:10.1126/science.288.5473.2028

Marra, J. 2002. Approaches to the measurement of plankton production, p. 78–108. *In* P. J. le. B. Williams, D. N. Thomas, and C. S. Reynolds [eds.], Phytoplankton productivity: Carbon assimilation in marine and freshwater ecosystems. Blackwell Science.

McClain, C. R., M. L. Cleave, G. C. Feldman, W. W. Gregg, S. B. Hooker, and N. Kuring. 1998. Science quality SeaWiFS data for global biosphere research. Sea Technol. **39:** 10–16.

Morel, A., and S. Maritorena. 2001. Bio-optical properties of oceanic waters: A reappraisal. J. Geophys. Res. **104:** 7163–7180, doi:10.1029/2000JC000319

Nicholson, D., S. Emerson, and C. C. Eriksen. 2008. Net community production in the deep euphotic zone of the subtropical North Pacific gyre from glider surveys. Limnol. Oceanogr. **53:** 2226–2236, doi:10.4319/lo.2008.53.5_part_2.2226

Oviatt, C. A., P. H. Doering, B. L. Nowicki, and A. Zoppini. 1993. Net system production in coastal waters as a function of eutrophication, seasonality, and benthic macrofaunal abundance. Estuaries **16:** 247–253, doi:10.2307/1352497

Regaudie-de-Gioux, A., and C. M. Duarte. 2012. Temperature dependence of planktonic metabolism in the ocean. Global Biogeochem. Cycles **26:** GB1015, doi:10.1029/2010GB003907

———, and ———. 2013. Plankton metabolism in the ocean. Consejo Superior de Investigaciones Científicas, Barcelona. https://digital.csic.es/handle/10261/65674

Robinson, C., and P. J. le B. Williams. 2005. Respiration and its measurement in surface marine waters, p. 147–181. *In* P. A. del Giorgio and P. J. le B. Williams [eds.], Respiration in aquatic ecosystems. Oxford Univ. Press.

———, and others. 2009. Comparison of in vitro and in situ plankton production determinations. Aquat. Microb. Ecol. **54:** 13–34, doi:10.3354/ame01250

Spitzer, W. S., and W. J. Jenkins. 1989. Rates of vertical mixing, gas-exchange and new production—estimates from seasonal gas cycles in the upper ocean near Bermuda. J. Mar. Res. **47:** 169–196, doi:10.1357/002224089785076370

Steeman Nielsen, E. 1952. The use of radioactive carbon (^{14}C) for measuring production in the sea. J. Cons. Perm. Int. Explor. Mer. **18:** 117–140.

Taylor, D., S. Nixon, S. Granger, and B. Buckley. 1995. Nutrient limitation and the eutrophication of coastal lagoons. Mar. Ecol. Prog. Ser. **127:** 235–244, doi:10.3354/meps127235

Tengberg, A., and others. 2006. Evaluation of a lifetime-based optode to measure oxygen in aquatic systems. Limnol. Oceanogr.: Methods **4:** 7–17, doi:10.4319/lom.2006.4.7

Williams, P. J. le B., and D. G. Bower. 1999. Regional carbon imbalances in the oceans. Science **284:** 173–174, doi:10.1126/science.284.5421.1735b

———, P. D. Quay, T. K. Westberry, and M. J. Behrenfeld. 2013. The oligotrophic ocean is autotrophic. Annu. Rev. Mar. Sci. **5:** 535–549, doi:10.1146/annurev-marine-121211-172335

Associate editor: Jonathan J. Cole

Received: 03 April 2012
Accepted: 14 November 2012
Amended: 11 February 2013